AGU ADVANCING EARTH AND SPACE SCIENCE

Geophysical Research Letters®

RESEARCH LETTER
10.1029/2021GL095831

Quantifying Carbon Monoxide Emissions on the Scale of Large Wildfires

M. M. Bela[1,2], N. Kille[1,3,4], S. A. McKeen[1,2], J. Romero-Alvarez[1,3], R. Ahmadov[1,5], E. James[1,5], G. Pereira[6,7], C. Schmidt[8], R. B. Pierce[9], S. M. O'Neill[10], X. Zhang[11], S. Kondragunta[12], C. Wiedinmyer[1], and R. Volkamer[1,3,4]

[1]Cooperative Institute for Research in Environmental Sciences (CIRES), University of Colorado Boulder, Boulder, CO, USA, [2]NOAA Chemical Sciences Laboratory (CSL), Boulder, CO, USA, [3]Department of Chemistry, University of Colorado Boulder, Boulder, CO, USA, [4]Department of Atmospheric and Oceanic Sciences, University of Colorado Boulder, Boulder, CO, USA, [5]NOAA Global Systems Laboratory (GSL), Boulder, CO, USA, [6]Departamento de Geociências, Universidade Federal de São João del-Rei, São João del-Rei, Brasil, [7]Programa de Pós-graduação em Geografia Física, Universidade de São Paulo, São Paulo, Brasil, [8]Cooperative Institute for Meteorological Satellite Studies, Space Science and Engineering Center, University of Wisconsin-Madison, Madison, WI, USA, [9]Space Science and Engineering Center, University of Wisconsin-Madison, Madison, WI, USA, [10]Pacific Northwest Research Station, United States Forest Service (USFS), Seattle, WA, USA, [11]South Dakota State University, Brookings, SD, USA, [12]NOAA/NESDIS Center for Satellite Applications and Research, College Park, MD, USA

Abstract The University of Colorado Airborne Solar Occultation Flux (CU AirSOF) instrument conducted the first suborbital carbon monoxide (CO) mass flux measurements on the scale of large wildfires, showing that the destructive fires in northern California in October 2017 emitted 2,040 ± 316 tonnes CO hr^{-1}. Pyrogenic estimates from seven satellite-based emission inventories bracket the observed flux, but their range spans a factor of 83. The simulated air quality impacts in the form of ozone and fine particulate matter scale primarily with these uncertain emission amounts, and range from insignificant to very severe. This uncertainty in predicting emissions is reduced to a factor of ~2 by the CU AirSOF flux measurements, with potential for future improvements. The uncertainty is primarily the result of uncertain vegetation types and sources of radiative power measurements, and to a lesser extent uncertain emission factors and fire diurnal cycles.

Plain Language Summary Wildfire smoke is a major source of air pollution that affects public health and natural areas, but the amounts of vegetation that go up in smoke and the emitted amounts of smoke are not well known, due to a lack of direct measurements. The accuracy of models used to predict smoke impacts on public health in affected communities is significantly impacted by their reliance on uncertain emissions estimates. In this study, a new instrument, the University of Colorado Airborne Solar Occultation Flux (CU AirSOF), measured the amount of carbon monoxide (CO) produced by the destructive fires in northern California during October 2017. These are the first airborne emission measurements on the scale of a large wildfire. The measured CO emissions from the fires fall within the large range among satellite-based emission estimates, reducing the uncertainty in fire emissions. Air quality impacts in the form of ozone (O_3) and fine particulate matter ($PM_{2.5}$) range from insignificant to very severe, in direct relationship to the uncertain satellite-based emission estimates.

Key Points:

- First suborbital carbon monoxide flux measurements on the scale of large wildfires
- Carbon monoxide fire emission inventories span a factor of 83 for a case study day of the northern California fires in October 2017
- Predicted ozone and fine particulate matter impacts vary from insignificant to very severe depending primarily on uncertain emission amounts

Supporting Information:

Supporting Information may be found in the online version of this article.

Correspondence to:

R. Volkamer and M. M. Bela,
rainer.volkamer@colorado.edu;
megan.bela@noaa.gov

Citation:

Bela, M. M., Kille, N., McKeen, S. A., Romero-Alvarez, J., Ahmadov, R., James, E., et al. (2022). Quantifying carbon monoxide emissions on the scale of large wildfires. *Geophysical Research Letters*, *49*, e2021GL095831. https://doi.org/10.1029/2021GL095831

Received 20 SEP 2021
Accepted 23 DEC 2021

1. Introduction

The October 2017 fires near Santa Rosa in northern California (N. CA) were the second most destructive fires to date in California (CalFire, 2021), killing 44 people (Nauslar et al., 2018), destroying nearly 9,000 structures (Mass & Ovens, 2019; Nauslar et al., 2018), with reported losses of over $10 billion (Mass & Ovens, 2019), and resulting in the highest $PM_{2.5}$ levels recorded by regulatory monitors in the Bay Area Air District since 1999 (Alrick, 2019). The Tubbs fire, the largest of the October 2017 N. CA fires, which devastated the city of Santa Rosa, was started by a private electrical system (CalFire, 2021), and was associated with an intense terrain-induced downslope windstorm. Such windstorms, commonly known as North or Diablo winds, can be very destructive when driving fires (McClung & Mass, 2020), and are projected to extend the fire season later into the fall and winter as a result of climate change (Guzman-Morales & Gershunov, 2019).

The 2018 Camp Fire, the deadliest and most destructive fire in CA history to date, was sparked by power lines (CalFire, 2021). The October 2017 N. CA fires and the Camp Fire are examples of fires with anthropogenic ignition sources and their subsequent air quality impacts that have broadened the spatial and seasonal reach of fire (Balch et al., 2017) and are likely to increase due to a warmer and drier climate in the Western U.S. during the 21st century (Flannigan et al., 2013; Mann et al., 2016; Moritz et al., 2012; Yue et al., 2013). These trends, combined with rising numbers of humans living in the urban-wildland interface, are likely to result in increases in population exposure to fire activity (Hammer et al., 2009; Huff et al., 2015) and poor air quality episodes (Liu et al., 2016). Long term exposure to elevated $PM_{2.5}$ may also increase human susceptibility to respiratory diseases such as coronavirus (COVID-19; Bourdrel et al., 2021; Henderson, 2020; Wu et al., 2020).

Pyrogenic emissions used as input for smoke and air quality forecasting models are often estimated from satellite data based on burned-area (EPA, 2020; Larkin et al., 2009; Longo et al., 2010; Wiedinmyer et al., 2011). An alternative approach exploits the empirically derived linear relation between the energy released as thermal radiation and the amount of fuel consumed during combustion (Ahmadov et al., 2017; Koster et al., 2015; Zhang et al., 2012). This approach relates Fire Radiative Energy (FRE, MJ), the time integral of Fire Radiative Power (FRP, J s^{-1}) observed from satellites, with the amount of biomass burned via a combustion factor β (kg dry matter MJ^{-1}; Freeborn et al., 2008; Kaiser et al., 2012; Wooster, 2002; Wooster et al., 2005), or with the amount of trace gas released into the atmosphere via a coefficient of emission C_e (g MJ^{-1}; Freeborn et al., 2008; Ichoku et al., 2008; Ichoku & Kaufman, 2005; Kremens et al., 2012; Li et al., 2018, 2020; Lu et al., 2019; Mota & Wooster, 2018).

The first deployment of the CU AirSOF instrument (Kille et al., 2022) quantified the emission fluxes of the N. CA wildfires on 10 October 2017. These are the first CO emission flux quantifications using airborne CO column measurements on the scale of actual wildfires. CU AirSOF is an appropriate tool to gather data on multiple wildfires (e.g., during the 2018 Biomass Burning Fluxes of Trace Gases and Aerosols (BB-FLUX) campaign; Volkamer et al., 2020) to generate regional and ecosystem specific averages for C_e and β.

In this study, we compare the CU AirSOF CO flux measurements for the October 2017 N. CA fires with estimates from seven satellite-based emission inventories. We combine the flux estimates with satellite FRP to calculate C_e and β, and compare with literature values. Finally, we use a regional chemical model to assess the sensitivity of predicted surface air quality impacts to emission amounts and diurnal cycle.

2. Methods

2.1. CU AirSOF Instrument

The CU AirSOF instrument (Kille et al., 2022) consists of a Fourier Transform Spectrometer installed on a research aircraft, and uses a custom-built digital fast solar tracker (Baidar et al., 2016) to point directly at the sun to measure trace gas vertical column densities (VCDs) above the aircraft at mid-infrared wavelengths. CU AirSOF is a further development of the ground-based CU mobile SOF instrument, which has been used to quantify emissions from area sources (Ibrahim et al., 2010; Kille et al., 2017, 2019; Mellqvist et al., 2010). Emission fluxes are calculated using the mass balance approach (Ibrahim et al., 2010; Kille et al., 2017; Mellqvist et al., 2010), in which VCD measurements and winds normal to the flight direction are integrated for each transect:

$$F_x = \frac{M_x}{N_A} \int \Delta VCD(s)\ \vec{u} \cdot \vec{n}(s)\ ds \tag{1}$$

where F_x is the emission flux (g s^{-1}) of species X (in this case, X is CO), M_{CO} is the CO molar mass (28 g mol^{-1}), N_A is Avogadro's number (molec mol^{-1}), ΔVCD is the enhanced CO column observation in the plume over background air (molec cm^{-2}), s is the aircraft path below the plume (cm), $\vec{u}$ is the average wind vector (cm s^{-1}) measured within the plume aboard the aircraft, and $\vec{n}(s)$ is the normal vector orthogonal to the aircraft direction.

The CU AirSOF instrument is a unique prototype (Kille et al., 2022) and is optimized to quantify wildfire emissions due to its ability to capture VCDs of trace gases above the aircraft through thick smoke plumes. CU AirSOF is conceptually similar to ground-based solar Fourier-transform infrared spectroscopy (FTIR) instruments, which provide long-term stationary column measurements at much higher spectral resolution relying on plume portions to pass over the instrument location (Lutsch et al., 2020; Paton-Walsh et al., 2004), but is optimized for mobile

aircraft deployment downwind of fires. On the other hand, flux estimation methods based on in-situ trace gas or aerosol sampling do not characterize the entire spatial extent of the plume, and are thus more affected by plume heterogeneity (Hodshire et al., 2019; Riggan et al., 2004). Satellite-based emission estimate methods, although providing global coverage multiple times a day or regional coverage throughout the day, may be limited by the coarse spatial resolution of observations.

2.2. CU AirSOF Measurements During the Precursor Biomass Burning Fluxes of Trace Gases and Aerosol Field Campaign (Pre-BB-FLUX)

Focused testing of CU AirSOF in biomass burning smoke took place on 10 October 2017, during Pre-BB-FLUX (http://flights.uwyo.edu/projects/prebbflux17/), targeting the smoke from the N. CA wildfires. The University of Wyoming King Air (UWKA) aircraft conducted two plume underpasses (T1 and T2) in the CA Central Valley at distances of ~60–100 km downwind of the fires, 2 hr apart in the early to mid-afternoon local time (Figure 1a). The plume was decoupled from the ground, as is indicated by the aerosol vertical profile measured shortly before T2 with the Passive Cavity Aerosol Spectrometer Probe (PCASP) aboard the UWKA (Figure 1b). The CO emission fluxes (Table 1) were calculated using Equation 1 for each plume underpass. Additional methods details, and the error budget for the CU AirSOF CO fluxes, are provided in Supporting Information S1.

Figure 1d shows the spectral proof of CO detection by observing the uniquely specific fingerprint absorption in the mid infrared region (4,215–4,254 cm^{-1}) in solar spectra (700–5,000 cm^{-1}) measured through the smoke plume. The CO column signal varies by a factor of 2.7 at constant altitude (~300 m above ground level) inside and outside of the plume (Figure 1c). The CO fingerprint absorption is well separated from other trace gases that are fitted simultaneously in this spectral region (Figure S1 in Supporting Information S1). Furthermore, the CO column sensitivity of CU AirSOF above the aircraft is independent of altitude (Figure S2 in Supporting Information S1).

2.3. Satellite FRP and C_e Values

FRP observed by the Geostationary Operational Environmental Satellite (GOES)-16 Advanced Baseline Imager (ABI; Schmidt, 2020) and Near Real Time Aqua and Terra Moderate Resolution Imaging Spectroradiometer (MODIS; Giglio et al., 2016) sensors was used to calculate C_e and β values, and were compared with that from the Visible Infrared Imaging Radiometer Suite (VIIRS) aboard the Suomi National Polar-orbiting Partnership (NPP; Csiszar et al., 2014). GOES-16 and MODIS made measurements close to the T1 (GOES-16) and T2 (GOES-16, MODIS) emissions times. GOES-16 FRP observations with any quality flag were used.

The CO C_e (g CO MJ^{-1}) was calculated as the ratio of the CU AirSOF fluxes (g CO s^{-1}) and satellite FRP (MJ s^{-1}):

$$C_e = \frac{F_{CO}}{FRP} \tag{2}$$

and β (kg dry matter MJ^{-1}) was calculated as:

$$\beta = \frac{F_{CO}}{EF \cdot FRP} \tag{3}$$

where EF is the CO emission factor (g CO (kg dry matter)$^{-1}$). Satellite FRP observations were summed over the N. CA fire region (37.86°N to 41.05°N, 123.46°W to 122.23°W).

2.4. Meteorology-Chemistry Simulations

Online coupled meteorology-chemistry simulations from 5 p.m. Pacific Daylight Time (PDT) on 9 October 2017 to 11 p.m. PDT on 10 October 2017, with 4 km horizontal grid spacing covering the N. CA fire region, were conducted using the Weather Research and Forecasting coupled with Chemistry (WRF-Chem) model (Skamarock et al., 2005) v. 3.9.1.1. Additional details (Bahreini et al., 2018; Freitas et al., 2007; Guenther et al., 2006; McDonald et al., 2018; Stockwell et al., 1997; Tuccella et al., 2015) are contained in Supporting Information S1.

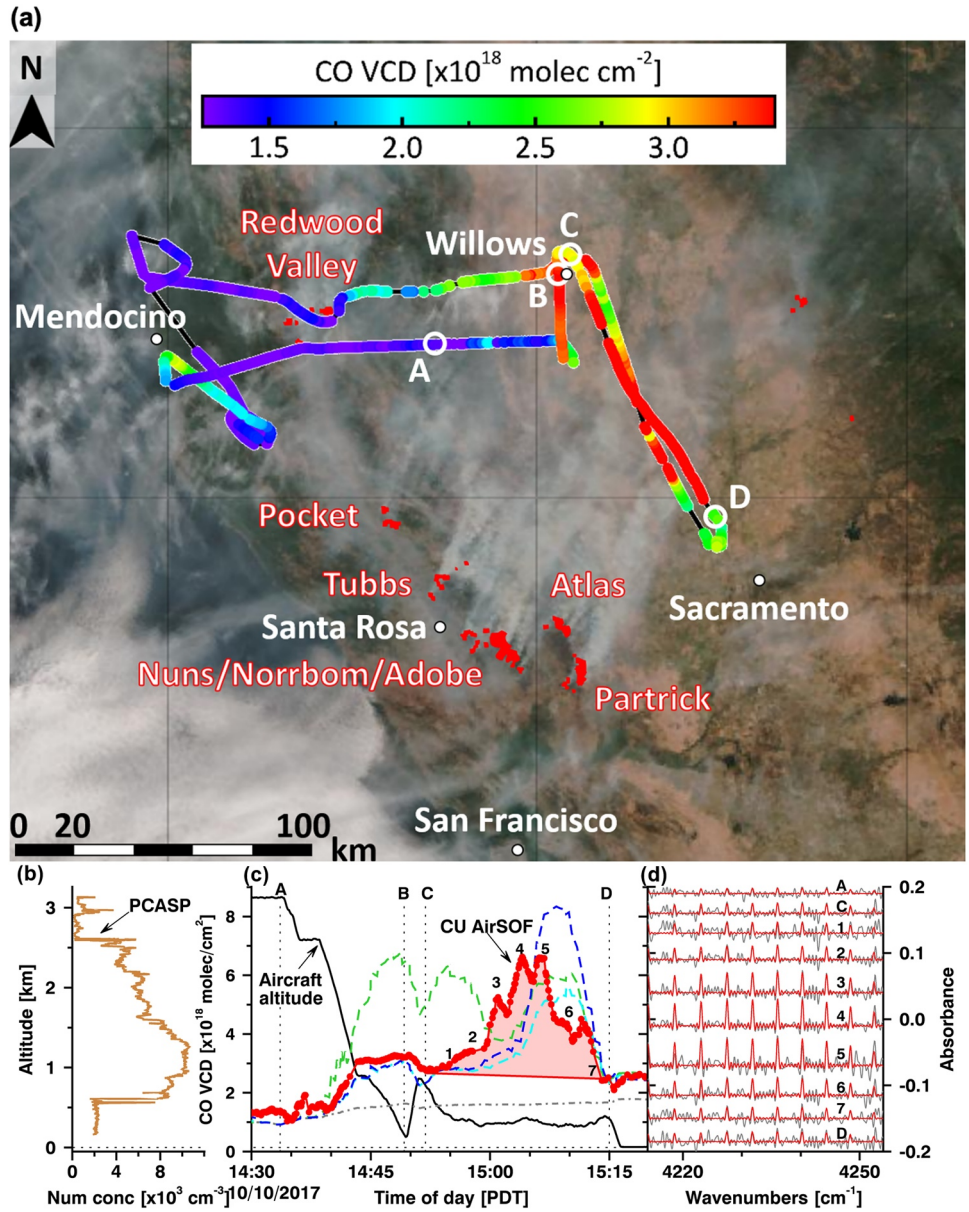

Figure 1. (a) Flight track on 10 October 2017 color coded with CO VCDs measured by CU AirSOF, overlaid on VIIRS satellite image (14:11 PDT); cities (white dots), fire locations (red dots), locations of labels shown in (c) (white open circles). (b) Aerosol number concentration vertical profile from Passive Cavity Aerosol Spectrometer Probe (PCASP) near Willow, CA. (c) CO from CU AirSOF (red) and WRF-Chem simulations: no pyrogenic emissions (gray); emissions constrained by T2 CU AirSOF flux with constant emissions (green), or using climatological (blue) or GOES-16 (cyan) diurnal cycles. (d) Spectral proof of CO fingerprint absorption outside (A, D) and inside (1–7) the plume, showing scaled CO reference spectrum (red) overlaid with residual noise (gray). Location and time period of vertical profile (A to B) and T2 period (C to D).

In the WRF-Chem simulations, total emissions of CO were set equal to either the CU AirSOF CO constrained daily mean emission mass flux of 2,884 tonnes hr^{-1}, or values spanning the orders of magnitude of the satellite-based emissions (10; 830; or 10,000 tonnes hr^{-1}). The emission time of the plume sampled during T2 was estimated using aging tracers in the WRF-Chem simulations. The CU AirSOF CO constrained daily mean mass flux was determined by integrating a diurnal cycle derived by fitting daily Gaussian functions to GOES-16 FRP (i.e., as in Mu et al. (2011); Figure S3 in Supporting Information S1), for the first 24 hr, with the emissions scaled to 2,040 tonnes hr^{-1} at the T2 emissions time, then dividing the scaled integrated emissions by 24 hr. Emissions of other

Table 1
Pyrogenic CO Emissions and C_e and β^a Values Based on CU AirSOF Measurements, at T1 and T2 Emissions Times

	AirSOF CO emissions (tonnes hr^{-1})	FRP J s^{-1}		C_e (g CO MJ^{-1})		β^a (kg dry matter MJ^{-1})	
		GOES-16 (15 min mean)	MODIS	GOES-16	MODIS	GOES-16	MODIS
T1	425 ± 137	7.07×10^8	–	167 ± 54	–	2.42 ± 0.78	–
T2	2,040 ± 316	3.80×10^9	7.78×10^9	149 ± 23	73 ± 11	2.16 ± 0.33	1.06 ± 0.16

[a]CO EF of 69 g kg^{-1}, the mean value for savannah/grassland (Andreae, 2019), was used.

gases and aerosols were scaled to the CO emissions via EFs (Andreae & Merlet, 2001; Yokelson et al., 2013). All pyrogenic emissions were distributed temporally either (a) at a constant rate, (b) varying over the course of the simulation according to a climatological diurnal cycle (Air Sciences, 2018; Figure S3 in Supporting Information S1), or (c) varying according to the GOES-16 FRP derived diurnal cycle. The error budget for adjusting the CU AirSOF fluxes into the model emissions is given in Supporting Information S1.

3. Results and Discussion

3.1. Measured and Satellite-Based Emissions

The N. CA fires depicted in Figure 1 emitted 2,040 ± 316 tonnes hr^{-1} of CO on 10 October 2017 (Table 1), as calculated from the CU AirSOF measurements. Model inventory daily mean values (see Supporting Information S1) vary by a factor of 83 among the 9 estimates, which range from 79 to 6,570 tonnes hr^{-1} of CO (Figure 2 and Table S1 in Supporting Information S1). The uncertainty in predicting pyrogenic CO emissions is reduced to a factor of ~2 by the CU AirSOF technique (Table 1). A previous comparison of four satellite-based inventories found monthly CO emissions for the continental United States (CONUS) for most of 2006 varied up to factor of 10 (Al-Saadi et al., 2008), and another comparing six satellite-based inventories showed organic carbon emissions in temperate North America for 2008 spanned a factor of 17 (Pan et al., 2020). Another study noted that North American biomass burning aerosol emissions for 2004–2016 from four satellite-based inventories varied by a factor of 4–7 (Carter et al., 2020).

The CU AirSOF fluxes fall within the range of satellite-based inventories extrapolated to the transect emissions times according to the GOES-16 or climatological diurnal cycles (Table S1 in Supporting Information S1). Variations due to the choice of diurnal cycle used to extrapolate satellite-based emissions to CU AirSOF emission

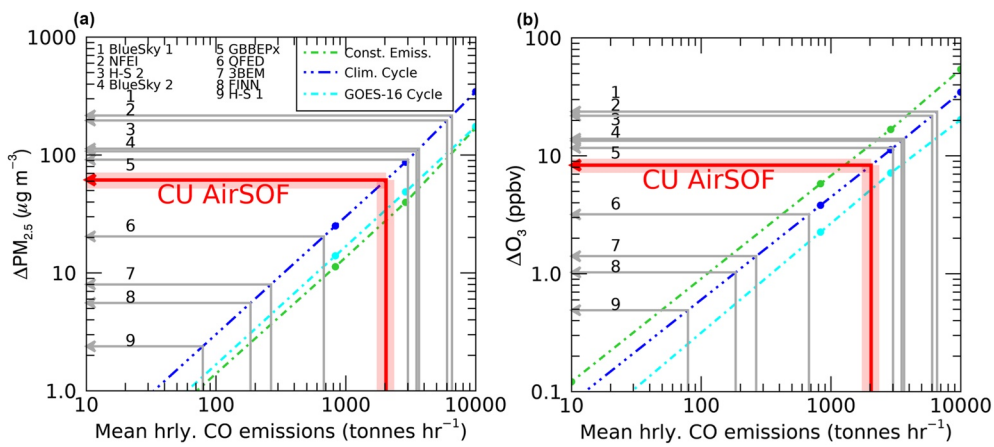

Figure 2. Air quality implications (horizontal lines) of uncertainties in fire emissions (vertical lines) quantified as mean PBL changes in October 2017 N. CA fires region at 3 p.m. PDT on 10 October 2017 in (a) $PM_{2.5}$ concentration and (b) O_3 mixing ratio simulated by WRF-Chem using constant and diurnally varying fire emissions. CU AirSOF T2 CO emission flux (red lines with red shading indicating 1 σ uncertainties) and hourly mean pyrogenic CO emissions from satellite inventories (gray lines; "H-S" designates HRRR-Smoke).

times are much smaller (within a factor of 2, Table S1 in Supporting Information S1) than the overall variability among the emission inventories.

3.2. C_e and β Values

C_e was found to be 167 ± 54 g CO MJ^{-1} (using GOES-16 FRP) for T1, and 73 ± 11 g CO MJ^{-1} (using MODIS FRP) or 149 ± 23 g CO MJ^{-1} (using GOES-16 FRP) for T2 (Table 1). We find the overall uncertainty in adjusting the CU AirSOF fluxes into the model emissions to be 65%, higher than the 16%–32% uncertainty in the CU AirSOF fluxes (see Supporting Information S1 for uncertainty calculations), but much lower than the factor of 83 variation in satellite-based emissions. The CU AirSOF CO fluxes increased from T1 to T2 by a factor of ∼5, reflecting the intensifying fire activity. However, the C_e value differs by only 12% between the two transect sampling periods when using GOES-16 FRP (Table 1). MODIS FRP yields a different C_e from values estimated using GOES-16 for the second transect time by a factor of 2, pointing to the need to evaluate the satellite FRP data, and determine how to best combine data from polar-orbiting satellites, which offer higher spatial resolution but are snapshots in time, with geostationary observations, which better capture the rapid variations of fire emissions.

Our C_e values for the savannah and forest fuels (identified by the Fuel Characteristic Classification System (FCCS; Ottmar et al., 2007); see Table S2 in Supporting Information S1) burned in the October 2017 N. CA fires are bracketed by those measured in burn chambers (Table S2 in Supporting Information S1). The broad agreement with literature C_e values is promising, but is based on a single case study flight, and should be viewed as a qualitative demonstration of concept.

Measuring C_e directly using the CU AirSOF method combined with high resolution vegetation and fuel datasets, such as were gathered during the BB-FLUX campaign (Volkamer et al., 2020), allow the evaluation of burned-area-based satellite emission methods that depend on vegetation and fuel maps to calculate emissions using EFs and fuel consumption, which has been widely measured in the field for different ecosystems (Akagi et al., 2011; Campbell et al., 2007; van Leeuwen et al., 2014). In the simplified vegetation classification used in models, the October 2017 N. CA fires are categorized as containing both savannah and extratropical forest fuels, for which CO EF values range by a factor of 3, and β values vary by a factor of 2 (Table S2 in Supporting Information S1). This variability in EF and β values is relevant for modeling because both fuel types must be represented in order to accurately characterize emissions. CO EFs are also strongly controlled by the relative proportions of flaming and smoldering combustion, commonly reported as the modified combustion efficiency (MCE; Andreae, 2019). However, if the vegetation type is unknown, CO EF values vary by a factor of 13, and β values by a factor of 45 (Table S2 in Supporting Information S1). By contrast, the FRP value from the MODIS instrument is a factor of 2 higher than those from GOES-16 at the T2 emissions time (Table 1), which is consistent with a previous study that demonstrated the ability of MODIS to detect smaller and cooler fires due to its higher spatial resolution than GOES (Li et al., 2019).

The variability in emissions among inventories (a factor of 83) is significantly larger than the variations in FRP, β, or EF, particularly if the correct ecosystem type is known. Thus, we infer that uncertain satellite-based emissions on 10 October 2017 for the N. CA fires are primarily the result of uncertain vegetation types, and to a lesser extent uncertain EFs, FRP, and diurnal cycles.

3.3. Simulated Smoke Transport

While the uncertainty in the CO mass flux as calculated using CU AirSOF is rather low (T1: 32.2%, T2: 15.5%; see Supporting Information S1), comparison with the modeled CO columns is affected by the need to correct for atmospheric transport and by uncertainties in the satellite-detected fire location, fire intensity (FRP), and diurnal cycle used to model the fire emissions (65%; see Supporting Information S1). The results are also impacted by the vertical distribution of the emissions, which we did not evaluate in this study.

We focus on the T2 aircraft sampling time, since T1 also sampled recirculated air containing emissions from the previous night, as determined from the model simulations, when we do not have emissions observations. WRF-Chem simulations better reproduce the CU AirSOF observations of CO VCDs using emissions with a climatological or GOES-16-based diurnal cycle rather than constant emissions (Figure 1c). A constant emission rate results in CO accumulation in the model, due to model emissions that were higher than the diurnally varying emissions

during a period of stagnation in wind circulation, which results in overestimates of the observed CO VCDs at the T2 aircraft sampling time (Figure 2). We conclude that in order to best simulate the atmospheric state observed by CU AirSOF, the measured emission flux needs to be constrained in the model, and the fire diurnal cycle must be properly represented.

Air quality and smoke forecasting models typically use either a constant or climatological diurnal cycle, but could benefit from using diurnal cycles based on high temporal resolution satellite FRP observations (e.g., GOES-16 for the U.S.). For example, nocturnal emissions from the 2013 CA Rim Fire determined by an inverse modeling method constrained by airborne in-situ CO were a factor of 10 times higher than a climatological diurnal cycle would predict (Saide et al., 2015). Furthermore, for WRF–Community Multiscale Air Quality Modeling System simulations of the October 2017 N. CA fires, it was necessary to use 5-min temporal resolution GOES-R FRP to shape the diurnal cycle of hourly emissions in order to reproduce smoke impacts from the rapidly increasing fire activity in the first 12 hr after initiation (O'Neill et al., 2021). Nevertheless, forecasting the temporal variability of fire emissions remains a significant challenge for current operational atmospheric models.

3.4. Sensitivity of Air Quality to Emissions

The October 2017 N. CA fires adversely impacted air quality in the Bay Area. Although surface aerosol number concentrations were low in the T2 sampling region (Figure 1b), surface $PM_{2.5}$ reached up to 280 μg m^{-3} $PM_{2.5}$ (very unhealthy levels) in the nearby city of Santa Rosa on this case study day (US EPA), and up to 440 μg m^{-3} in the city of Vallejo on 11 October 2017 (Alrick, 2019). Model-predicted air quality impacts from wildfires are particularly sensitive to emitted amounts of CO, which are tightly bound here by the CU AirSOF fluxes, since CO is used widely to represent emissions of other pollutants via vegetation-dependent EFs, as was done in this study.

The change in mean $PM_{2.5}$ concentrations and O_3 mixing ratios in the planetary boundary layer (PBL) between simulations with and without fire emissions at the T2 time in the October 2017 N. CA fire region were calculated for WRF-Chem simulations with mean hourly CO emissions spanning the 2 orders of magnitude of the satellite-based inventories (Figure 2 and Figure S4 in Supporting Information S1). Mean boundary layer values are shown in order to separate the effects of emissions amounts and diurnal cycle, as model inaccuracies in vertical mixing and PBL height, the assessment of which is outside the scope of this work, may result in errors in surface concentrations. Figure 2 shows that the production of O_3 and $PM_{2.5}$ averaged over the fire region exhibits a linear relationship with wildfire emissions on the regional scale. The mean PBL $PM_{2.5}$ and O_3 vary by 2 orders of magnitude in simulations with CO emissions spanning a similar range, representative of the large spread among satellite-based inventories. By comparison, diurnal cycle effects are small. Only a factor of 2 change is seen in predicted $PM_{2.5}$ and O_3 between model runs with constant versus diurnally varied emissions. The air quality impacts of the N. CA fires predicted by the climatological diurnal cycle simulation range from negligible (0.03 μg m^{-3} $PM_{2.5}$ and 0.01 ppbv O_3) to severe for $PM_{2.5}$ (345 μg m^{-3} $PM_{2.5}$ and 35 ppbv O_3), depending primarily on the emission amounts. The WRF-Chem simulations do not include aerosol radiative impacts on photolysis rates. O_3 production may be increased close to fires, but reduced downwind due to high $PM_{2.5}$ loadings (Jiang et al., 2012; McClure & Jaffe, 2018).

Our results highlight the importance of accurate emissions amounts, which can be experimentally constrained from CU AirSOF measurements, for predicting wildfire air quality impacts.

4. Summary and Conclusions

Our case study of the N. CA wildfires on 10 October 2017 illustrates the large impact of these fires on air quality. CU AirSOF provides a promising new tool that has begun to be utilized to investigate ecosystem-atmosphere linkages (BB-FLUX campaign; Volkamer et al., 2020). Quantifying emission mass fluxes by CU AirSOF is not limited to CO, but has been extended to measurements of other trace gases that absorb light at mid-infrared wavelengths (Kille et al., 2022). The CU AirSOF measurements enable the calculation of the emission coefficient C_e from satellite FRP, now provided at high frequency by geostationary measurements. C_e values determined from MODIS and GOES-16 FRP for the 10 October 2017 N. CA wildfires differ by a factor of 2. Differences in FRP from polar-orbiting and geostationary satellites need to be reconciled in order to accurately constrain emissions. For a case study day of the October 2017 N. CA fires, emissions amounts, rather than their temporal distribution, are the primary drivers of model uncertainty in simulated O_3 production from wildfire emissions. Uncertain mass

fluxes from satellite-based emissions inventories in this study are primarily the result of uncertain ecosystem types, but are also affected by fire regimes and behavior, and by uncertainties in the satellite FRP data. More direct flux measurements are needed to establish a robust relationship between CO emissions and satellite FRP, and to assess the variability of C_e for different fuel types and burn conditions. Fuel and vegetation maps with high spatial and temporal resolution and global coverage are needed for any satellite-based emissions approach to work broadly.

This study also indicates that estimating emissions from polar-orbiting instrument observations alone (Figure S3 in Supporting Information S1) would lead to large errors in fire intensity, but by using the climatological diurnal cycle the error is reduced acceptably.

The amounts of O_3, $PM_{2.5}$, and other pollutants that are produced from wildfire emissions remain highly uncertain. North American wildfires have been observed to both efficiently generate and suppress O_3 (Jaffe & Wigder, 2012). Current research and operational air quality forecasting models tend to overestimate O_3 production from wildfires (Baker et al., 2018). In addition to affecting air quality directly, aerosols from fires absorb and scatter solar radiation and provide condensation nuclei for clouds, impacting weather forecast parameters (e.g., surface temperature, precipitation), public health, life, property, and climate (Grell et al., 2011; Grell & Freitas, 2014; Jiang et al., 2012). Better constraints on C_e may lead to improved operational air quality and weather model predictions.

Data Availability Statement

The Pre-BB-FLUX data set is available from https://data.eol.ucar.edu/project/Pre-BB-FLUX, via https://doi.org/10.26023/VC8N-ZJ4H-HQ0A (CU AirSOF data), and https://doi.org/10.26023/KR9Z-2JQG-DB12 (Supplementary Sensor Data). VIIRS NPP FRP data are available at https://dx.doi.org/10.5067/VIIRS/VNP14.001, Fire INventory from NCAR (National Center for Atmospheric Research; FINN) v1.5 emissions at https://www.acom.ucar.edu/Data/fire/, National Fire Emissions Inventory (NFEI) at https://www.epa.gov/air-emissions-inventories/2017-national-emissions-inventory-nei-data, Quick Fire Emissions Data set v2.5r1 (QFED) at http://ftp.as.harvard.edu/gcgrid/data/ExtData/HEMCO/QFED/v2018-07/2017/10/, the first USFS estimate at https://haze.airfire.org/webaccess/susan/HAQAST/Wildfires_TT/FireEmissionInventory/OLD_preliminary/fire_locations_20171010-NapaFires.csv, and the second USFS estimate at https://haze.airfire.org/webaccess/susan/HAQAST/Wildfires_TT/FireEmissionInventory/Baseline/fire_locations_20171008_step1out.csv. The WRF-Chem v.3.9.1.1 source code is available via https://doi.org/10.5065/D6MK6B4K. The model meteorological input data are available at https://www.ncdc.noaa.gov/has/HAS.FileAppRouter?datasetname=NAMANL218&subqueryby=STATION&applname=&outdest=FILE for North American Mesoscale Analysis, https://www.ecmwf.int/en/forecasts/datasets/reanalysis-datasets/era-interim for European Centre for Medium-Range Weather Forecasts Re-Analysis Interim, https://doi.org/10.5065/D65D8PWK for Global Forecast System, and https://www.ncei.noaa.gov/products/weather-climate-models/rapid-refresh-update for Rapid Refresh. All other data are available at https://csl.noaa.gov/groups/csl4/modeldata/data/Bela2021/.

Acknowledgments
The Pre-BB-FLUX field campaign was supported by NSF awards AGS-1744537 and AGS-1754019 (PI: Rainer Volkamer). This work was supported in part by the NOAA Cooperative Agreement with CIRES, NA17OAR4320101. Natalie Kille received a CIRES Graduate Student Research Award. The authors thank the Pre-BB-FLUX science team, especially Barbara Dix and David Thomson, and the UW flight center staff, especially Matt Burkhart, Brent Glover, Ben Heesen, Bill Kuestner, Zane Little, Nick Mahon, Larry Oolman, and Brett Wadsworth. The authors thank Gregory Frost and Robert Yokelson for feedback on the manuscript, Robert Lipschutz (NOAA/GSL) for the RAP and GFS meteorological and MODIS FRP data, and Ivan Csiszar and Marina Tsidulko for the VIIRS FRP data. R. Ahmadov and E. James thank NOAA's JPSS Proving Ground and Risk Reduction program for funding.

References

Ahmadov, R., Grell, G. A., James, E., Alexander, C., Stewart, J., Benjamin, S., & Goldberg, M. (2017). Using JPSS VIIRS fire radiative power data to forecast biomass burning emissions and smoke transport by the High Resolution Rapid Refresh Model. In *2017 IEEE International Geoscience and Remote Sensing Symposium (IGARSS)* (pp. 2806–2808). Retrieved from https://ui.adsabs.harvard.edu/abs/2017AGUFMIN53D

Air Sciences, I. (2018). *Integrated assessment update and 2018 emissions inventory for prescribed fire, wildfire, and agricultural burning*. Western Governors Association/Western Regional Air Partnership/Fire Emissions Joint Forum. Retrieved from https://www.wrapair.org/forums/fejf/documents/emissions/WGA2018report20051123

Akagi, S. K., Yokelson, R. J., Wiedinmyer, C., Alvarado, M. J., Reid, J. S., Karl, T., et al. (2011). Emission factors for open and domestic biomass burning for use in atmospheric models. *Atmospheric Chemistry and Physics*, *11*(9), 4039–4072. https://doi.org/10.5194/acp-11-4039-2011

Alrick, D. (2019). The October 2017 North Bay Fires: Applying new observational and prediction tools to smoke and air quality forecasting. *Paper presented at 99th American Meteorological Society Annual Meeting*. Phoenix, AZ.

Al-Saadi, J. A., Soja, A. J., Pierce, R. B., Szykman, J. J., Wiedinmyer, C., Emmons, L. K., & Bowman, K. W. (2008). Intercomparison of near-real-time biomass burning emissions estimates constrained by satellite fire data. *Journal of Applied Remote Sensing*, 2(1), 1–24. https://doi.org/10.1117/1.294878510.1117/1.2948785

Andreae, M. O. (2019). Emission of trace gases and aerosols from biomass burning—An updated assessment. *Atmospheric Chemistry and Physics*, *19*(13), 8523–8546. https://doi.org/10.5194/acp-19-8523-2019

Andreae, M. O., & Merlet, P. (2001). Emission of trace gases and aerosols from biomass burning. *Global Biogeochemical Cycles*, *15*(4), 955–966. https://doi.org/10.1029/2000gb001382

Bahreini, R., Ahmadov, R., McKeen, S. A., Vu, K. T., Dingle, J. H., Apel, E. C., et al. (2018). Sources and characteristics of summertime organic aerosol in the Colorado Front Range: Perspective from measurements and WRF-Chem modeling. *Atmospheric Chemistry and Physics*, *18*(11), 8293–8312. https://doi.org/10.5194/acp-18-8293-2018

Baidar, S., Kille, N., Ortega, I., Sinreich, R., Thomson, D., Hannigan, J., & Volkamer, R. (2016). Development of a digital mobile solar tracker. *Atmospheric Measurement Techniques*, *9*(3), 963–972. https://doi.org/10.5194/amt-9-963-2016

Baker, K. R., Woody, M. C., Valin, L., Szykman, J., Yates, E. L., Iraci, L. T., et al. (2018). Photochemical model evaluation of 2013 California wild fire air quality impacts using surface, aircraft, and satellite data. *Science of the Total Environment*, *637–638*, 1137–1149. https://doi.org/10.1016/j.scitotenv.2018.05.048

Balch, J. K., Bradley, B. A., Abatzoglou, J. T., Nagy, R. C., Fusco, E. J., & Mahood, A. L. (2017). Human-started wildfires expand the fire niche across the United States. *Proceedings of the National Academy of Sciences*, *114*(11), 2946–2951. https://doi.org/10.1073/pnas.1617394114

Bourdrel, T., Annesi-Maesano, I., Alahmad, B., Maesano, C. N., & Bind, M.-A. (2021). The impact of outdoor air pollution on COVID-19: A review of evidence from in vitro, animal, and human studies. *European Respiratory Review*, *30*(159). https://doi.org/10.1183/16000617.0242-2020

CalFire. (2021). *Top 20 most destructive California wildfires*. Retrieved From https://www.fire.ca.gov/media/t1rdhizr/top20_destruction.pdf

Campbell, J., Donato, D., Azuma, D., & Law, B. (2007). Pyrogenic carbon emission from a large wildfire in Oregon, United States. *Journal of Geophysical Research*, *112*(G4). https://doi.org/10.1029/2007jg000451

Carter, T. S., Heald, C. L., Jimenez, J. L., Campuzano-Jost, P., Kondo, Y., Moteki, N., et al. (2020). How emissions uncertainty influences the distribution and radiative impacts of smoke from fires in North America. *Atmospheric Chemistry and Physics*, *20*(4), 2073–2097. https://doi.org/10.5194/acp-20-2073-2020

Csiszar, I., Schroeder, W., Giglio, L., Ellicott, E., Vadrevu, K. P., Justice, C. O., & Wind, B. (2014). Active fires from the Suomi NPP visible infrared imaging radiometer suite: Product status and first evaluation results. *Journal of Geophysical Research: Atmospheres*, *119*(2), 803–816. https://doi.org/10.1002/2013jd020453

EPA. (2020). *National Emissions Inventory (NEI) 2017, Version 1. (Technical Report)*. Research Triangle Park, N.C., Office of Air Quality Planning and Standards. U.S. Environmental Protection Agency

Flannigan, M., Cantin, A. S., de Groot, W. J., Wotton, M., Newbery, A., & Gowman, L. M. (2013). Global wildland fire season severity in the 21st century. *Forest Ecology and Management*, *294*, 54–61. https://doi.org/10.1016/j.foreco.2012.10.02

Freeborn, P. H., Wooster, M. J., Hao, W. M., Ryan, C. A., Nordgren, B. L., Baker, S. P., & Ichoku, C. (2008). Relationships between energy release, fuel mass loss, and trace gas and aerosol emissions during laboratory biomass fires. *Journal of Geophysical Research*, *113*(D1). https://doi.org/10.1029/2007jd008679

Freitas, S. R., Longo, K. M., Chatfield, R., Latham, D., Silva Dias, M. A. F., Andreae, M. O., et al. (2007). Including the sub-grid scale plume rise of vegetation fires in low resolution atmospheric transport models. *Atmospheric Chemistry and Physics*, *7*(13), 3385–3398. https://doi.org/10.5194/acp-7-3385-2007

Giglio, L., Schroeder, W., & Justice, C. O. (2016). The collection 6 MODIS active fire detection algorithm and fire products. *Remote Sensing of Environment*, *178*, 31–41. https://doi.org/10.1016/j.rse.2016.02.054

Grell, G., & Freitas, S. R. (2014). A scale and aerosol aware stochastic convective parameterization for weather and air quality modeling. *Atmospheric Chemistry and Physics*, *14*(10), 5233–5250. https://doi.org/10.5194/acp-14-5233-2014

Grell, G., Freitas, S. R., Stuefer, M., & Fast, J. (2011). Inclusion of biomass burning in WRF-Chem: Impact of wildfires on weather forecasts. *Atmospheric Chemistry and Physics*, *11*(11), 5289–5303. https://doi.org/10.5194/acp-11-5289-2011

Guenther, A., Karl, T., Harley, P., Wiedinmyer, C., Palmer, P. I., & Geron, C. (2006). Estimates of global terrestrial isoprene emissions using MEGAN (Model of Emissions of Gases and Aerosols from Nature). *Atmospheric Chemistry and Physics*, *6*(11), 3181–3210. https://doi.org/10.5194/acp-6-3181-2006

Guzman-Morales, J., & Gershunov, A. (2019). Climate change suppresses Santa Ana Winds of Southern California and sharpens their seasonality. *Geophysical Research Letters*, *46*(5), 2772–2780. https://doi.org/10.1029/2018GL080261

Hammer, R. B., Stewart, S. I., & Radeloff, V. C. (2009). Demographic trends, the wildland–urban interface, and wildfire management. *Society & Natural Resources*, *22*(8), 777–782. https://doi.org/10.1080/08941920802714042

Henderson, S. B. (2020). The COVID-19 pandemic and wildfire smoke: Potentially concomitant disasters. *American Journal of Public Health*, *110*(8), 1140–1142. https://doi.org/10.2105/AJPH.2020.305744

Hodshire, A. L., Bian, Q., Ramnarine, E., Lonsdale, C. R., Alvarado, M. J., Kreidenweis, S. M., et al. (2019). More than emissions and chemistry: Fire size, dilution, and background aerosol also greatly influence near-field biomass burning aerosol aging. *Journal of Geophysical Research: Atmospheres*, *124*(10), 5589–5611. https://doi.org/10.1029/2018jd029674

Huff, A. K., Kondragunta, S., Zhang, H., & Hoff, R. M. (2015). Monitoring the impacts of wildfires on forest ecosystems and public health in the exo-urban environment using high-resolution satellite aerosol products from the Visible Infrared Imaging Radiometer Suite (VIIRS). *Environmental Health Insights*, *9*, 9–18. https://doi.org/10.4137/EHI.S19590

Ibrahim, O., Shaiganfar, R., Sinreich, R., Stein, T., Platt, U., & Wagner, T. (2010). Car MAX-DOAS measurements around entire cities: Quantification of NO_x emissions from the cities of Mannheim and Ludwigshafen (Germany). *Atmospheric Measurement Techniques*, *3*(3), 709–721. https://doi.org/10.5194/amt-3-709-2010

Ichoku, C., & Kaufman, Y. (2005). A method to derive smoke emission rates from MODIS fire radiative energy measurements. *IEEE Transactions on Geoscience and Remote Sensing*, *43*(11), 2636–2649. https://doi.org/10.1109/TGRS.2005.857328

Ichoku, C., Martins, J. V., Kaufman, Y. J., Wooster, M. J., Freeborn, P. H., Hao, W. M., & Nordgren, B. L. (2008). Laboratory investigation of fire radiative energy and smoke aerosol emissions. *Journal of Geophysical Research*, *113*(D14). https://doi.org/10.1029/2007jd009659

Jaffe, D. A., & Wigder, N. L. (2012). Ozone production from wildfires: A critical review. *Atmospheric Environment*, *51*, 1–10. https://doi.org/10.1016/j.atmosenv.2011.11.063

Jiang, X., Wiedinmyer, C., & Carlton, A. G. (2012). Aerosols from fires: An examination of the effects on ozone photochemistry in the Western United States. *Environmental Science & Technology*, *46*(21), 11878–11886. https://doi.org/10.1021/es301541k10.1021/es301541k

Kaiser, J. W., Heil, A., Andreae, M. O., Benedetti, A., Chubarova, N., Jones, L., et al. (2012). Biomass burning emissions estimated with a global fire assimilation system based on observed fire radiative power. *Biogeosciences*, *9*(1), 527–554. https://doi.org/10.5194/bg-9-527-2012

Kille, N., Baidar, S., Handley, P., Ortega, I., Sinreich, R., Cooper, O. R., et al. (2017). The CU mobile Solar Occultation Flux instrument: Structure functions and emission rates of NH_3, NO_2 and C_2H_6. *Atmospheric Measurement Techniques*, *10*(1), 373–392. https://doi.org/10.5194/amt-10-373-2017

Kille, N., Chiu, R., Frey, M., Hase, F., Sha, M. K., Blumenstock, T., et al. (2019). Separation of methane emissions from agricultural and natural gas sources in the Colorado Front Range. *Geophysical Research Letters*, *46*(7), 3990–3998. https://doi.org/10.1029/2019gl082132

Kille, N., Zarzana, K. J., Romero Alvarez, J., Lee, C. F., Rowe, J. P., Howard, B., et al. (2022). The CU airborne solar occultation flux instrument: Performance evaluation during BB-flux. *ACS Earth and Space Chemistry*. https://doi.org/10.1021/acsearthspacechem.1c00281

Koster, R. D., Darmenov, A. S., & da Silva, A. M. (2015). *The Quick Fire Emissions Dataset (QFED): Documentation of versions 2.1, 2.2 and 2.4 (Tech. Rep.)*. Retrieved from https://ntrs.nasa.gov/citations/20180005253

Kremens, R. L., Dickinson, M. B., & Bova, A. S. (2012). Radiant flux density, energy density and fuel consumption in mixed-oak forest surface fires. *International Journal of Wildland Fire*, *21*(6), 722–730. https://doi.org/10.1071/wf10143

Larkin, N. K., O'Neill, S. M., Solomon, R., Raffuse, S., Strand, T., Sullivan, D. C., et al. (2009). The BlueSky smoke modeling framework. *International Journal of Wildland Fire*, *18*(8), 906–920. https://doi.org/10.1071/wf07086

Li, F., Zhang, X., Kondragunta, S., & Lu, X. (2020). An evaluation of advanced baseline imager fire radiative power based wildfire emissions using carbon monoxide observed by the Tropospheric Monitoring Instrument across the conterminous United States. *Environmental Research Letters*, *15*(9), 094049. https://doi.org/10.1088/1748-9326/ab9d3a

Li, F., Zhang, X., Kondragunta, S., & Roy, D. P. (2018). Investigation of the fire radiative energy biomass combustion coefficient: A comparison of polar and geostationary satellite retrievals over the conterminous United States. *Journal of Geophysical Research: Biogeosciences*, *123*(2), 722–739. https://doi.org/10.1002/2017jg004279

Li, F., Zhang, X., Roy, D. P., & Kondragunta, S. (2019). Estimation of biomass-burning emissions by fusing the fire radiative power retrievals from polar-orbiting and geostationary satellites across the conterminous United States. *Atmospheric Environment*, *211*, 274–287. https://doi.org/10.1016/j.atmosenv.2019.05.017

Liu, J. C., Mickley, L. J., Sulprizio, M. P., Dominici, F., Yue, X., Ebisu, K., et al. (2016). Particulate air pollution from wildfires in the Western US under climate change. *Climatic Change*, *138*, 655–666. https://doi.org/10.1007/s10584-016-1762-6

Longo, K. M., Freitas, S. R., Andreae, M. O., Setzer, A., Prins, E., & Artaxo, P. (2010). The coupled aerosol and tracer transport model to the Brazilian developments on the Regional Atmospheric Modeling System (CATT-BRAMS)—Part 2: Model sensitivity to the biomass burning inventories. *Atmospheric Chemistry and Physics*, *10*(13), 5785–5795. https://doi.org/10.5194/acp-10-5785-2010

Lu, X., Zhang, X., Li, F., & Cochrane, M. A. (2019). Investigating smoke aerosol emission coefficients using MODIS active fire and aerosol products: A case study in the CONUS and Indonesia. *Journal of Geophysical Research: Biogeosciences*, *124*(6), 1413–1429. https://doi.org/10.1029/2018jg004974

Lutsch, E., Strong, K., Jones, D. B. A., Blumenstock, T., Conway, S., Fisher, J. A., et al. (2020). Detection and attribution of wildfire pollution in the Arctic and northern midlatitudes using a network of Fourier-transform infrared spectrometers and GEOS-Chem. *Atmospheric Chemistry and Physics*, *20*(21), 12813–12851. https://doi.org/10.5194/acp-20-12813-2020

Mann, M. L., Batllori, E., Moritz, M. A., Waller, E. K., Berck, P., Flint, A. L., et al. (2016). Incorporating anthropogenic influences into fire probability models: Effects of human activity and climate change on fire activity in California. *PLoS One*, *11*(4), 1–21. https://doi.org/10.1371/journal.pone.0153589

Mass, C. F., & Ovens, D. (2019). The Northern California Wildfires of 8–9 October 2017: The role of a major downslope wind event. *Bulletin of the American Meteorological Society*, *100*(2), 235–256. https://doi.org/10.1175/bams-d-18-0037.1

McClung, B., & Mass, C. F. (2020). The strong, dry winds of Central and Northern California: Climatology and synoptic evolution. *Weather and Forecasting*, *35*(5), 2163–2178. https://doi.org/10.1175/waf-d-19-0221.1

McClure, C. D., & Jaffe, D. A. (2018). Investigation of high ozone events due to wildfire smoke in an urban area. *Atmospheric Environment*, *194*, 146–157. https://doi.org/10.1016/j.atmosenv.2018.09.021

McDonald, B. C., McKeen, S. A., Cui, Y. Y., Ahmadov, R., Kim, S.-W., Frost, G. J., et al. (2018). Modeling ozone in the Eastern U.S. using a fuel-based mobile source emissions inventory. *Environmental Science & Technology*, *52*(13), 7360–7370. https://doi.org/10.1021/acs.est.8b0077810.1021/acs.est.8b00778

Mellqvist, J., Samuelsson, J., Johansson, J., Rivera, C., Lefer, B., Alvarez, S., & Jolly, J. (2010). Measurements of industrial emissions of alkenes in Texas using the solar occultation flux method. *Journal of Geophysical Research*, *115*(D7). https://doi.org/10.1029/2008jd011682

Moritz, M. A., Parisien, M.-A., Batllori, E., Krawchuk, M. A., Van Dorn, J., Ganz, D. J., & Hayhoe, K. (2012). Climate change and disruptions to global fire activity. *Ecosphere*, *3*(6), art49. https://doi.org/10.1890/es11-00345.1

Mota, B., & Wooster, M. J. (2018). A new top-down approach for directly estimating biomass burning emissions and fuel consumption rates and totals from geostationary satellite fire radiative power (FRP). *Remote Sensing of Environment*, *206*, 45–62. https://doi.org/10.1016/j.rse.2017.12.016

Mu, M., Randerson, J. T., van der Werf, G. R., Giglio, L., Kasibhatla, P., Morton, D., & Wennberg, P. O. (2011). Daily and 3-hourly variability in global fire emissions and consequences for atmospheric model predictions of carbon monoxide. *Journal of Geophysical Research*, *116*(D24). https://doi.org/10.1029/2011jd016245

Nauslar, N. J., Abatzoglou, J. T., & Marsh, P. T. (2018). The 2017 North Bay and Southern California fires: A case study. *Fire*, *1*(1), 18. https://doi.org/10.3390/fire1010018

O'Neill, S. M., Diao, M., Raffuse, S., Al-Hamdan, M., Barik, M., Jia, Y., et al. (2021). A multi-analysis approach for estimating regional health impacts from the 2017 Northern California wildfires. *Journal of the Air & Waste Management Association*, *71*(7), 791–814. https://doi.org/10.1080/10962247.2021.1891994

Ottmar, R. D., Sandberg, D. V., Riccardi, C. L., & Prichard, S. J. (2007). An overview of the Fuel Characteristic Classification System—Quantifying, classifying, and creating fuelbeds for resource planning. *Canadian Journal of Forest Research*, *37*(12), 2383–2393. https://doi.org/10.1139/X07-077

Pan, X., Ichoku, C., Chin, M., Bian, H., Darmenov, A., Colarco, P., et al. (2020). Six global biomass burning emission datasets: Intercomparison and application in one global aerosol model. *Atmospheric Chemistry and Physics*, *20*(2), 969–994. https://doi.org/10.5194/acp-20-969-2020

Paton-Walsh, C., Jones, N., Wilson, S., Meier, A., Deutscher, N., Griffith, D., & Campbell, S. (2004). Trace gas emissions from biomass burning inferred from aerosol optical depth. *Geophysical Research Letters*, *31*(5). https://doi.org/10.1029/2003gl018973

Riggan, P. J., Tissell, R. G., Lockwood, R. N., Brass, J. A., Pereira, J. A. R., Miranda, H. S., et al. (2004). Remote measurement of energy and carbon flux from wildfires in Brazil. *Ecological Applications*, *14*(3), 855–872. https://doi.org/10.1890/02-5162

Saide, P. E., Peterson, D. A., Silva, A. d., Anderson, B., Ziemba, L. D., Diskin, G., et al. (2015). Revealing important nocturnal and day-to-day variations in fire smoke emissions through a multiplatform inversion. *Geophysical Research Letters*, *42*(9), 3609–3618. https://doi.org/10.1002/2015gl063737

Schmidt, C. (2020). Chapter 13: Monitoring fires with the GOES-R series In Goodman, S. J., Schmit, T. J., Daniels, J., & Redmon, R. J. (Eds.), *The GOES-R series: A new generation of geostationary environmental satellites* (pp. 145–163). Elsevier. https://doi.org/10.1016/B978-0-12-814327-8.00013-5

Skamarock, W. C., Klemp, J. B., Dudhia, J., Gill, D. O., Barker, D. M., Wang, W., & Powers, J. G. (2005). *A description of the Advanced Research WRF Version 2 (No. NCAR/TN-468+STR) (Tech. Rep.)*. University Corporation for Atmospheric Research. https://doi.org/10.5065/D6DZ069T

Stockwell, W., Kirchner, F., Kuhn, M., & Seefeld, S. (1997). A new mechanism for regional atmospheric chemistry modeling. *Journal of Geophysical Research*, *102*, 25847–25879. https://doi.org/10.1029/97JD00849

Tuccella, P., Curci, G., Grell, G. A., Visconti, G., Crumeyrolle, S., Schwarzenboeck, A., & Mensah, A. A. (2015). A new chemistry option in WRF-Chem v. 3.4 for the simulation of direct and indirect aerosol effects using VBS: Evaluation against IMPACT-EUCAARI data. *Geoscientific Model Development*, *8*(9), 2749–2776. https://doi.org/10.5194/gmd-8-2749-2015

van Leeuwen, T. T., van der Werf, G. R., Hoffmann, A. A., Detmers, R. G., Rücker, G., French, N. H. F., et al. (2014). Biomass burning fuel consumption rates: A field measurement database. *Biogeosciences*, *11*(24), 7305–7329. https://doi.org/10.5194/bg-11-7305-2014

Volkamer, R., Kille, N., Lee, C. F., Zarzana, K. J., Koenig, T., Nutter, R., & Ottmar, R. D. (2020). The BB-FLUX Project: How much fuel goes up in smoke? *Invited talk presented at American Meteorological Society 100th Annual Meeting*. Boston, MA. https://ams.confex.com/ams/2020Annual/videogateway.cgi/id/522007?recordingid=522007

Wiedinmyer, C., Akagi, S. K., Yokelson, R. J., Emmons, L. K., Al-Saadi, J. A., Orlando, J. J., & Soja, A. J. (2011). The Fire INventory from NCAR (FINN): A high resolution global model to estimate the emissions from open burning. *Geoscientific Model Development*, *4*(3), 625–641. https://doi.org/10.5194/gmd-4-625-2011

Wooster, M. J. (2002). Small-scale experimental testing of fire radiative energy for quantifying mass combusted in natural vegetation fires. *Geophysical Research Letters*, *29*(21). https://doi.org/10.1029/2002gl015487

Wooster, M. J., Roberts, G., Perry, G. L. W., & Kaufman, Y. J. (2005). Retrieval of biomass combustion rates and totals from fire radiative power observations: FRP derivation and calibration relationships between biomass consumption and fire radiative energy release. *Journal of Geophysical Research*, *110*(D24). https://doi.org/10.1029/2005jd006318

Wu, X., Nethery, R. C., Sabath, M. B., Braun, D., & Dominici, F. (2020). Air pollution and COVID-19 mortality in the United States: Strengths and limitations of an ecological regression analysis. *Science Advances*, *6*(45). https://doi.org/10.1126/sciadv.abd4049

Yokelson, R. J., Burling, I. R., Gilman, J. B., Warneke, C., Stockwell, C. E., de Gouw, J., et al. (2013). Coupling field and laboratory measurements to estimate the emission factors of identified and unidentified trace gases for prescribed fires. *Atmospheric Chemistry and Physics*, *13*(1), 89–116. https://doi.org/10.5194/acp-13-89-2013

Yue, X., Mickley, L. J., Logan, J. A., & Kaplan, J. O. (2013). Ensemble projections of wildfire activity and carbonaceous aerosol concentrations over the western United States in the mid-21st century. *Atmospheric Environment*, *77*, 767–780. https://doi.org/10.1016/j.atmosenv.2013.06.003

Zhang, X., Kondragunta, S., Ram, J., Schmidt, C., & Huang, H.-C. (2012). Near-real-time global biomass burning emissions product from geostationary satellite constellation. *Journal of Geophysical Research*, *117*(D14). https://doi.org/10.1029/2012jd017459